PHYSICAL REVIEW D **85,** 011102(R) (2012)

Search for $\bar{B} \to \Lambda_c^+ X \ell^- \bar{\nu}_\ell$ decays in events with a fully reconstructed B meson

J. P. Lees,[1] V. Poireau,[1] V. Tisserand,[1] J. Garra Tico,[2] E. Grauges,[2] M. Martinelli,[3a,3b] D. A. Milanes,[3a] A. Palano,[3a,3b] M. Pappagallo,[3a,3b] G. Eigen,[4] B. Stugu,[4] L. Sun,[4] D. N. Brown,[5] L. T. Kerth,[5] Yu. G. Kolomensky,[5] G. Lynch,[5] T. Tanabe,[5] H. Koch,[6] T. Schroeder,[6] D. J. Asgeirsson,[7] C. Hearty,[7] T. S. Mattison,[7] J. A. McKenna,[7] A. Khan,[8] V. E. Blinov,[9] A. R. Buzykaev,[9] V. P. Druzhinin,[9] V. B. Golubev,[9] E. A. Kravchenko,[9] A. P. Onuchin,[9] S. I. Serednyakov,[9] Yu. I. Skovpen,[9] E. P. Solodov,[9] K. Yu. Todyshev,[9] A. N. Yushkov,[9] M. Bondioli,[10] D. Kirkby,[10] A. J. Lankford,[10] M. Mandelkern,[10] D. P. Stoker,[10] H. Atmacan,[11] J. W. Gary,[11] F. Liu,[11] O. Long,[11] G. M. Vitug,[11] C. Campagnari,[12] T. M. Hong,[12] D. Kovalskyi,[12] J. D. Richman,[12] C. A. West,[12] A. M. Eisner,[13] J. Kroseberg,[13] W. S. Lockman,[13] A. J. Martinez,[13] T. Schalk,[13] B. A. Schumm,[13] A. Seiden,[13] C. H. Cheng,[14] D. A. Doll,[14] B. Echenard,[14] K. T. Flood,[14] D. G. Hitlin,[14] P. Ongmongkolkul,[14] F. C. Porter,[14] A. Y. Rakitin,[14] R. Andreassen,[15] M. S. Dubrovin,[15] Z. Huard,[15] B. T. Meadows,[15] M. D. Sokoloff,[15] P. C. Bloom,[16] W. T. Ford,[16] A. Gaz,[16] M. Nagel,[16] U. Nauenberg,[16] J. G. Smith,[16] S. R. Wagner,[16] R. Ayad,[17,*] W. H. Toki,[17] B. Spaan,[18] M. J. Kobel,[19] K. R. Schubert,[19] R. Schwierz,[19] D. Bernard,[20] M. Verderi,[20] P. J. Clark,[21] S. Playfer,[21] D. Bettoni,[22a] C. Bozzi,[22a] R. Calabrese,[22a,22b] G. Cibinetto,[22a,22b] E. Fioravanti,[22a,22b] I. Garzia,[22a,22b] E. Luppi,[22a,22b] M. Munerato,[22a,22b] M. Negrini,[22a,22b] L. Piemontese,[22a] R. Baldini-Ferroli,[23] A. Calcaterra,[23] R. de Sangro,[23] G. Finocchiaro,[23] M. Nicolaci,[23] P. Patteri,[23] I. M. Peruzzi,[23,†] M. Piccolo,[23] M. Rama,[23] A. Zallo,[23] R. Contri,[24a,24b] E. Guido,[24a,24b] M. Lo Vetere,[24a,24b] M. R. Monge,[24a,24b] S. Passaggio,[24a] C. Patrignani,[24a,24b] E. Robutti,[24a] B. Bhuyan,[25] V. Prasad,[25] C. L. Lee,[26] M. Morii,[26] A. J. Edwards,[27] A. Adametz,[28] J. Marks,[28] U. Uwer,[28] F. U. Bernlochner,[29] M. Ebert,[29] H. M. Lacker,[29] T. Lueck,[29] P. D. Dauncey,[30] M. Tibbetts,[30] P. K. Behera,[31] U. Mallik,[31] C. Chen,[32] J. Cochran,[32] W. T. Meyer,[32] S. Prell,[32] E. I. Rosenberg,[32] A. E. Rubin,[32] A. V. Gritsan,[33] Z. J. Guo,[33] N. Arnaud,[34] M. Davier,[34] G. Grosdidier,[34] F. Le Diberder,[34] A. M. Lutz,[34] B. Malaescu,[34] P. Roudeau,[34] M. H. Schune,[34] A. Stocchi,[34] G. Wormser,[34] D. J. Lange,[35] D. M. Wright,[35] I. Bingham,[36] C. A. Chavez,[36] J. P. Coleman,[36] J. R. Fry,[36] E. Gabathuler,[36] D. E. Hutchcroft,[36] D. J. Payne,[36] C. Touramanis,[36] A. J. Bevan,[37] F. Di Lodovico,[37] R. Sacco,[37] M. Sigamani,[37] G. Cowan,[38] S. Paramesvaran,[38] D. N. Brown,[39] C. L. Davis,[39] A. G. Denig,[40] M. Fritsch,[40] W. Gradl,[40] A. Hafner,[40] E. Prencipe,[40] K. E. Alwyn,[41] D. Bailey,[41] R. J. Barlow,[41,‡] G. Jackson,[41] G. D. Lafferty,[41] R. Cenci,[42] B. Hamilton,[42] A. Jawahery,[42] D. A. Roberts,[42] G. Simi,[42] C. Dallapiccola,[43] R. Cowan,[44] D. Dujmic,[44] G. Sciolla,[44] D. Lindemann,[45] P. M. Patel,[45] S. H. Robertson,[45] M. Schram,[45] P. Biassoni,[46a,46b] A. Lazzaro,[46a,46b] V. Lombardo,[46a] N. Neri,[46a,46b] F. Palombo,[46a,46b] S. Stracka,[46a,46b] L. Cremaldi,[47] R. Godang,[47,§] R. Kroeger,[47] P. Sonnek,[47] D. J. Summers,[47] X. Nguyen,[48] P. Taras,[48] G. De Nardo,[49a,49b] D. Monorchio,[49a,49b] G. Onorato,[49a,49b] C. Sciacca,[49a,49b] G. Raven,[50] H. L. Snoek,[50] C. P. Jessop,[51] K. J. Knoepfel,[51] J. M. LoSecco,[51] W. F. Wang,[51] K. Honscheid,[52] R. Kass,[52] J. Brau,[53] R. Frey,[53] N. B. Sinev,[53] D. Strom,[53] E. Torrence,[53] E. Feltresi,[54a,54b] N. Gagliardi,[54a,54b] M. Margoni,[54a,54b] M. Morandin,[54a] M. Posocco,[54a] M. Rotondo,[54a] F. Simonetto,[54a,54b] R. Stroili,[54a,54b] E. Ben-Haim,[55] M. Bomben,[55] G. R. Bonneaud,[55] H. Briand,[55] G. Calderini,[55] J. Chauveau,[55] O. Hamon,[55] Ph. Leruste,[55] G. Marchiori,[55] J. Ocariz,[55] S. Sitt,[55] M. Biasini,[56a,56b] E. Manoni,[56a,56b] S. Pacetti,[56a,56b] A. Rossi,[56a,56b] C. Angelini,[57a,57b] G. Batignani,[57a,57b] S. Bettarini,[57a,57b] M. Carpinelli,[57a,57b,‖] G. Casarosa,[57a,57b] A. Cervelli,[57a,57b] F. Forti,[57a,57b] M. A. Giorgi,[57a,57b] A. Lusiani,[57a,57c] B. Oberhof,[57a,57b] E. Paoloni,[57a,57b] A. Perez,[57a] G. Rizzo,[57a,57b] J. J. Walsh,[57a] D. Lopes Pegna,[58] C. Lu,[58] J. Olsen,[58] A. J. S. Smith,[58] A. V. Telnov,[58] F. Anulli,[59a] G. Cavoto,[59a] R. Faccini,[59a,59b] F. Ferrarotto,[59a] F. Ferroni,[59a,59b] M. Gaspero,[59a,59b] L. Li Gioi,[59a] M. A. Mazzoni,[59a] G. Piredda,[59a] C. Bünger,[60] O. Grünberg,[60] T. Hartmann,[60] T. Leddig,[60] H. Schröder,[60] R. Waldi,[60] T. Adye,[61] E. O. Olaiya,[61] F. F. Wilson,[61] S. Emery,[62] G. Hamel de Monchenault,[62] G. Vasseur,[62] Ch. Yèche,[62] D. Aston,[63] D. J. Bard,[63] R. Bartoldus,[63] C. Cartaro,[63] M. R. Convery,[63] J. Dorfan,[63] G. P. Dubois-Felsmann,[63] W. Dunwoodie,[63] R. C. Field,[63] M. Franco Sevilla,[63] B. G. Fulsom,[63] A. M. Gabareen,[63] M. T. Graham,[63] P. Grenier,[63] C. Hast,[63] W. R. Innes,[63] M. H. Kelsey,[63] H. Kim,[63] P. Kim,[63] M. L. Kocian,[63] D. W. G. S. Leith,[63] P. Lewis,[63] S. Li,[63] B. Lindquist,[63] S. Luitz,[63] V. Luth,[63] H. L. Lynch,[63] D. B. MacFarlane,[63] D. R. Muller,[63] H. Neal,[63] S. Nelson,[63] I. Ofte,[63] M. Perl,[63] T. Pulliam,[63] B. N. Ratcliff,[63] A. Roodman,[63] A. A. Salnikov,[63] V. Santoro,[63] R. H. Schindler,[63] A. Snyder,[63] D. Su,[63] M. K. Sullivan,[63] J. Va'vra,[63] A. P. Wagner,[63] M. Weaver,[63] W. J. Wisniewski,[63] M. Wittgen,[63] D. H. Wright,[63] H. W. Wulsin,[63] A. K. Yarritu,[63] C. C. Young,[63] V. Ziegler,[63] W. Park,[64] M. V. Purohit,[64] R. M. White,[64] J. R. Wilson,[64] A. Randle-Conde,[65] S. J. Sekula,[65] M. Bellis,[66] J. F. Benitez,[66] P. R. Burchat,[66] T. S. Miyashita,[66] M. S. Alam,[67] J. A. Ernst,[67] R. Gorodeisky,[68] N. Guttman,[68] D. R. Peimer,[68] A. Soffer,[68] P. Lund,[69] S. M. Spanier,[69] R. Eckmann,[70] J. L. Ritchie,[70] A. M. Ruland,[70] C. J. Schilling,[70] R. F. Schwitters,[70] B. C. Wray,[70] J. M. Izen,[71] X. C. Lou,[71] F. Bianchi,[72a,72b] D. Gamba,[72a,72b] L. Lanceri,[73a,73b] L. Vitale,[73a,73b] F. Martinez-Vidal,[74] A. Oyanguren,[74] H. Ahmed,[75] J. Albert,[75] Sw. Banerjee,[75] H. H. F. Choi,[75]

G. J. King,[75] R. Kowalewski,[75] M. J. Lewczuk,[75] C. Lindsay,[75] I. M. Nugent,[75] J. M. Roney,[75] R. J. Sobie,[75] T. J. Gershon,[76] P. F. Harrison,[76] T. E. Latham,[76] E. M. T. Puccio,[76] H. R. Band,[77] S. Dasu,[77] Y. Pan,[77] R. Prepost,[77] C. O. Vuosalo,[77] and S. L. Wu[77]

(The *BABAR* Collaboration)

[1]*Laboratoire d'Annecy-le-Vieux de Physique des Particules (LAPP), Université de Savoie, CNRS/IN2P3, F-74941 Annecy-Le-Vieux, France*
[2]*Universitat de Barcelona, Facultat de Fisica, Departament ECM, E-08028 Barcelona, Spain*
[3a]*INFN Sezione di Bari, I-70126 Bari, Italy*
[3b]*Dipartimento di Fisica, Università di Bari, I-70126 Bari, Italy*
[4]*University of Bergen, Institute of Physics, N-5007 Bergen, Norway*
[5]*Lawrence Berkeley National Laboratory and University of California, Berkeley, California 94720, USA*
[6]*Ruhr Universität Bochum, Institut für Experimentalphysik 1, D-44780 Bochum, Germany*
[7]*University of British Columbia, Vancouver, British Columbia, Canada V6T 1Z1*
[8]*Brunel University, Uxbridge, Middlesex UB8 3PH, United Kingdom*
[9]*Budker Institute of Nuclear Physics, Novosibirsk 630090, Russia*
[10]*University of California at Irvine, Irvine, California 92697, USA*
[11]*University of California at Riverside, Riverside, California 92521, USA*
[12]*University of California at Santa Barbara, Santa Barbara, California 93106, USA*
[13]*University of California at Santa Cruz, Institute for Particle Physics, Santa Cruz, California 95064, USA*
[14]*California Institute of Technology, Pasadena, California 91125, USA*
[15]*University of Cincinnati, Cincinnati, Ohio 45221, USA*
[16]*University of Colorado, Boulder, Colorado 80309, USA*
[17]*Colorado State University, Fort Collins, Colorado 80523, USA*
[18]*Technische Universität Dortmund, Fakultät Physik, D-44221 Dortmund, Germany*
[19]*Technische Universität Dresden, Institut für Kern- und Teilchenphysik, D-01062 Dresden, Germany*
[20]*Laboratoire Leprince-Ringuet, Ecole Polytechnique, CNRS/IN2P3, F-91128 Palaiseau, France*
[21]*University of Edinburgh, Edinburgh EH9 3JZ, United Kingdom*
[22a]*INFN Sezione di Ferrara, I-44100 Ferrara, Italy*
[22b]*Dipartimento di Fisica, Università di Ferrara, I-44100 Ferrara, Italy*
[23]*INFN Laboratori Nazionali di Frascati, I-00044 Frascati, Italy*
[24a]*INFN Sezione di Genova, I-16146 Genova, Italy*
[24b]*Dipartimento di Fisica, Università di Genova, I-16146 Genova, Italy*
[25]*Indian Institute of Technology Guwahati, Guwahati, Assam, 781 039, India*
[26]*Harvard University, Cambridge, Massachusetts 02138, USA*
[27]*Harvey Mudd College, Claremont, California 91711*
[28]*Universität Heidelberg, Physikalisches Institut, Philosophenweg 12, D-69120 Heidelberg, Germany*
[29]*Humboldt-Universität zu Berlin, Institut für Physik, Newtonstr. 15, D-12489 Berlin, Germany*
[30]*Imperial College London, London, SW7 2AZ, United Kingdom*
[31]*University of Iowa, Iowa City, Iowa 52242, USA*
[32]*Iowa State University, Ames, Iowa 50011-3160, USA*
[33]*Johns Hopkins University, Baltimore, Maryland 21218, USA*
[34]*Laboratoire de l'Accélérateur Linéaire, IN2P3/CNRS et Université Paris-Sud 11, Centre Scientifique d'Orsay, B. P. 34, F-91898 Orsay Cedex, France*
[35]*Lawrence Livermore National Laboratory, Livermore, California 94550, USA*
[36]*University of Liverpool, Liverpool L69 7ZE, United Kingdom*
[37]*Queen Mary, University of London, London, E1 4NS, United Kingdom*
[38]*University of London, Royal Holloway and Bedford New College, Egham, Surrey TW20 0EX, United Kingdom*
[39]*University of Louisville, Louisville, Kentucky 40292, USA*
[40]*Johannes Gutenberg-Universität Mainz, Institut für Kernphysik, D-55099 Mainz, Germany*
[41]*University of Manchester, Manchester M13 9PL, United Kingdom*
[42]*University of Maryland, College Park, Maryland 20742, USA*
[43]*University of Massachusetts, Amherst, Massachusetts 01003, USA*
[44]*Massachusetts Institute of Technology, Laboratory for Nuclear Science, Cambridge, Massachusetts 02139, USA*
[45]*McGill University, Montréal, Québec, Canada H3A 2T8*
[46a]*INFN Sezione di Milano, I-20133 Milano, Italy*
[46b]*Dipartimento di Fisica, Università di Milano, I-20133 Milano, Italy*
[47]*University of Mississippi, University, Mississippi 38677, USA*

[48]Université de Montréal, Physique des Particules, Montréal, Québec, Canada H3C 3J7
[49a]INFN Sezione di Napoli, I-80126 Napoli, Italy
[49b]Dipartimento di Scienze Fisiche, Università di Napoli Federico II, I-80126 Napoli, Italy
[50]NIKHEF, National Institute for Nuclear Physics and High Energy Physics, NL-1009 DB Amsterdam, The Netherlands
[51]University of Notre Dame, Notre Dame, Indiana 46556, USA
[52]Ohio State University, Columbus, Ohio 43210, USA
[53]University of Oregon, Eugene, Oregon 97403, USA
[54a]INFN Sezione di Padova, I-35131 Padova, Italy
[54b]Dipartimento di Fisica, Università di Padova, I-35131 Padova, Italy
[55]Laboratoire de Physique Nucléaire et de Hautes Energies, IN2P3/CNRS, Université Pierre et Marie Curie-Paris6, Université Denis Diderot-Paris7, F-75252 Paris, France
[56a]INFN Sezione di Perugia, I-06100 Perugia, Italy
[56b]Dipartimento di Fisica, Università di Perugia, I-06100 Perugia, Italy
[57a]INFN Sezione di Pisa, I-56127 Pisa, Italy
[57b]Dipartimento di Fisica, Università di Pisa, I-56127 Pisa, Italy
[57c]Scuola Normale Superiore di Pisa, I-56127 Pisa, Italy
[58]Princeton University, Princeton, New Jersey 08544, USA
[59a]INFN Sezione di Roma, I-00185 Roma, Italy
[59b]Dipartimento di Fisica, Università di Roma La Sapienza, I-00185 Roma, Italy
[60]Universität Rostock, D-18051 Rostock, Germany
[61]Rutherford Appleton Laboratory, Chilton, Didcot, Oxon, OX11 0QX, United Kingdom
[62]CEA, Irfu, SPP, Centre de Saclay, F-91191 Gif-sur-Yvette, France
[63]SLAC National Accelerator Laboratory, Stanford, California 94309 USA
[64]University of South Carolina, Columbia, South Carolina 29208, USA
[65]Southern Methodist University, Dallas, Texas 75275, USA
[66]Stanford University, Stanford, California 94305-4060, USA
[67]State University of New York, Albany, New York 12222, USA
[68]Tel Aviv University, School of Physics and Astronomy, Tel Aviv, 69978, Israel
[69]University of Tennessee, Knoxville, Tennessee 37996, USA
[70]University of Texas at Austin, Austin, Texas 78712, USA
[71]University of Texas at Dallas, Richardson, Texas 75083, USA
[72a]INFN Sezione di Torino, I-10125 Torino, Italy
[72b]Dipartimento di Fisica Sperimentale, Università di Torino, I-10125 Torino, Italy
[73a]INFN Sezione di Trieste, I-34127 Trieste, Italy
[73b]Dipartimento di Fisica, Università di Trieste, I-34127 Trieste, Italy
[74]IFIC, Universitat de Valencia-CSIC, E-46071 Valencia, Spain
[75]University of Victoria, Victoria, British Columbia, Canada V8W 3P6
[76]Department of Physics, University of Warwick, Coventry CV4 7AL, United Kingdom
[77]University of Wisconsin, Madison, Wisconsin 53706, USA

(Received 27 October 2011; published 12 January 2012)

We present a search for semileptonic B decays to the charmed baryon Λ_c^+ based on 420 fb^{-1} of data collected at the $\Upsilon(4S)$ resonance with the *BABAR* detector at the PEP-II e^+e^- storage rings. By fully reconstructing the recoiling B in a hadronic decay mode, we reduce non-B backgrounds and determine the flavor of the signal B. We statistically correct the flavor for the effect of the B^0 mixing. We obtain a 90% confidence level upper limit of $\mathcal{B}(\bar{B} \to \Lambda_c^+ X \ell^- \bar{\nu}_\ell)/\mathcal{B}(\bar{B} \to \Lambda_c^+ X) < 3.5\%$.

DOI: 10.1103/PhysRevD.85.011102 PACS numbers: 13.20.He, 12.38.Qk, 14.40.Nd

Decays of B mesons to charmed baryons are not as well understood as those to charmed mesons. In particular, there is limited knowledge, both theoretical and experimental, about semileptonic $\bar{B}$ decays to the Λ_c^+ charmed baryon [1]. If $\bar{B}$ decays to charmed baryons are dominated by external W emission [Fig. 1(a)], as is the case for $\bar{B}$ decays to charmed mesons [2,3], and final-state hadronic interactions are small, the semileptonic fraction of these decays should be roughly the same:

$$\frac{\mathcal{B}(\bar{B} \to \Lambda_c^+ X \ell^- \bar{\nu}_\ell)}{\mathcal{B}(\bar{B} \to \Lambda_c^+ X')} \sim \frac{\mathcal{B}(\bar{B} \to D X'' \ell^- \bar{\nu}_\ell)}{\mathcal{B}(\bar{B} \to D X''')}, \quad (1)$$

*Now at Temple University, Philadelphia, PA 19122, USA.
†Also with Università di Perugia, Dipartimento di Fisica, Perugia, Italy.
‡Now at the University of Huddersfield, Huddersfield HD1 3DH, UK.
§Now at University of South Alabama, Mobile, AL 36688, USA.
‖Also with Università di Sassari, Sassari, Italy.

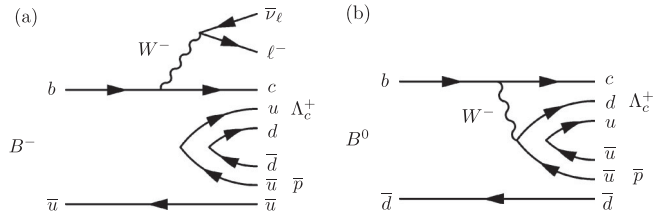

FIG. 1. Feynman diagrams for B decays into a charmed baryon through external W emission (a) and internal W emission (b).

where $\ell = e$ or μ, and D is understood to be $D^{(*)0}$ or $D^{(*)+}$. The semileptonic fraction of B decays to charmed mesons is currently measured to be $11.1 \pm 0.8\%$ [4]. A significantly smaller semileptonic ratio for B decays to charmed baryons would be evidence for a sizable internal W emission amplitude in baryonic B decay [Fig. 1(b)] or a large contribution of final-state interactions.

About 90% of the measured inclusive semileptonic $\bar{B} \to X_c \ell^- \bar{\nu}_\ell$ branching fraction into charmed final states can be accounted for by summing the branching fractions from exclusive $\bar{B} \to D^{(*)}(\pi)\ell^- \bar{\nu}_\ell$ decays [3]. Semileptonic B decays to charmed baryons could account for some of the remaining difference.

A previous search for semileptonic B decays into charmed baryons by the CLEO Collaboration [5] resulted in an upper limit on the ratio $\mathcal{B}(\bar{B} \to \Lambda_c^+ X e^- \bar{\nu}_e)/\mathcal{B}(B/\bar{B} \to \Lambda_c^+ X) < 5\%$ at the 90% confidence level. By using $\mathcal{B}(B/\bar{B} \to \Lambda_c^+ X) = 0.045 \pm 0.004 \pm 0.012$ and $\mathcal{B}(\bar{B} \to \bar{\Lambda}_c^- X)/\mathcal{B}(\bar{B} \to \Lambda_c^+ X) = 0.19 \pm 0.13 \pm 0.04$ [4], and assuming lepton universality, this result implies a semileptonic fraction limit $\mathcal{B}(\bar{B} \to \Lambda_c^+ X \ell^- \bar{\nu}_\ell)/\mathcal{B}(\bar{B} \to \Lambda_c^+ X) < 6\%$ at 90% confidence level.

There are two caveats to the CLEO measurement. First, the electron candidate is required to have a momentum greater than 0.6 GeV/c, which reduces background due to fake and secondary electrons, but may also reduce signal efficiency. Second, because the CLEO measurement was unable to constrain the flavor of the $\bar{B}$ meson, the quoted fraction suffers from large systematic uncertainties due to the uncorrelated $\bar{B} \to \bar{\Lambda}_c^- X$ background. We address these two points by reconstructing a B meson in a hadronic mode and look for the signal in its recoil. The resulting sample has less background, which allows us to lower the lepton momentum cutoff, and the flavor of the hadronic B meson determines the flavor of the signal $\bar{B}$, up to mixing effects. By normalizing to the correlated $\bar{B} \to \Lambda_c^+ X$ decay mode, many systematic uncertainties cancel.

In this paper, we present a search for semileptonic $\bar{B}$ decays to Λ_c^+ using data collected with the *BABAR* detector at the PEP-II asymmetric-energy e^+e^- storage rings at SLAC. The data consist of a total of 420 fb^{-1} recorded at the $\Upsilon(4S)$ resonance between 1999 and 2008, corresponding to approximately 460×10^6 $B\bar{B}$ pairs. The *BABAR* detector is described in detail elsewhere [6]. Charged particle trajectories are measured by a five-layer double-sided silicon vertex tracker and a 40-layer drift chamber, both operating in a 1.5 T magnetic field. Charged particle identification is provided by the specific ionization energy loss (dE/dx) in the tracking devices and by an internally reflecting ring-imaging Cherenkov detector. Photons are detected by a CsI(Tl) electromagnetic calorimeter . Muons are identified by the instrumented magnetic-flux return. A detailed GEANT4-based Monte Carlo (MC) simulation [7] of $B\bar{B}$ and continuum events (light quarks and τ pairs) is used to study the detector response, its acceptance, and to test the analysis techniques.

We search for semileptonic $\bar{B} \to \Lambda_c^+ X \ell^- \bar{\nu}_\ell$ decays with $\ell = e$ or μ in events preselected to contain a candidate B reconstructed in a fully hadronic decay mode ($B_{\rm tag}$), as described later in the text. We select signal candidates in these events by looking for candidate leptons and fully reconstructed Λ_c^+ decays. We then refine our selection of $B_{\rm tag}$, and make a final signal extraction based on the selected $B_{\rm tag}$ and Λ_c^+ kinematic properties. We also select candidate $\bar{B} \to \Lambda_c^+ X$ events, starting with the same sample and using similar techniques and selections, but without requiring an identified lepton candidate.

Selection criteria are optimized using MC simulation of signal and background processes. Because little is known about $\bar{B} \to \Lambda_c^+ X \ell^- \bar{\nu}_\ell$ decays, we use a signal model which can be tuned to cover a large range of possible kinematics of the final-state particles. In this model, the $\bar{B}$ decays semileptonically into an intermediate massive particle Y, $\bar{B} \to Y \ell^- \bar{\nu}_\ell$, with a kinematic distribution according to phase space [8]. The Y subsequently decays into a Λ_c^+, an antinucleon (antiproton or antineutron), and n_1 (n_2) charged (neutral) pions, again assuming phase space distributions. The free parameters in the model (the mass m_Y and width Γ_Y of the pseudoparticle Y, and n_1 and n_2) are tuned to reproduce the lepton and charmed hadron momentum spectra predicted by the $\bar{B} \to D^{(*)} \pi \ell \bar{\nu}_\ell$ model of Goity and Roberts [9], after accounting for the phase space limits implied by the large baryon masses. We choose $m_Y = 4.5$ GeV/c^2, $\Gamma_Y = 0.2$ GeV/c^2, and $n_1 + n_2 \leq 6$.

We reconstruct $B_{\rm tag}$ decays of the type $B \to \bar{D} Y'$, where Y' represents a collection of hadrons with a total charge of ± 1, composed of $n_1' \pi^\pm + n_2' K^\pm + n_3' K_S^0 + n_4' \pi^0$, where $n_1' + n_2' \leq 5$, $n_3' \leq 2$, and $n_4' \leq 2$. K_S^0 candidates are reconstructed in the $\pi^+\pi^-$ decay mode, π^0 candidates in the $\gamma\gamma$ mode. Using $\bar{D}^0(D^-)$ and $\bar{D}^{*0}(D^{*-})$ as seeds for $B^+(B^0)$ decays, we reconstruct about 1000 complete B decay chains [10].

The kinematic consistency of a $B_{\rm tag}$ candidate with a B meson decay is evaluated using two variables: the beam-energy substituted mass $m_{ES} \equiv \sqrt{s/4 - |p_B^*|^2}$, and the energy difference $\Delta E \equiv E_B^* - \sqrt{s}/2$. Here $\sqrt{s}$ is the total center of mass (CM) energy, and p_B^* and E_B^* denote the momentum and energy of the $B_{\rm tag}$ candidate in the CM frame. For correctly identified $B_{\rm tag}$ decays, the m_{ES}

distribution peaks at the B meson mass, with a resolution of about 2.5 MeV/c^2 averaged over the decay modes, while ΔE is consistent with zero, with a resolution of about 18 MeV. We select $B_{\rm tag}$ candidates in the signal region defined as $5.27\ {\rm GeV}/c^2 < m_{ES} < 5.29\ {\rm GeV}/c^2$, with a ΔE within 4σ of zero. This selection has an estimated efficiency of 0.2% to 0.3% per B meson.

We identify electron and muon candidates by combining the information on the measured momentum and energy loss in the silicon vertex tracker and drift chamber, the angle of Cherenkov radiation in the internally reflecting ring-imaging Cherenkov detector, and the energy deposition and shower shape in the electromagnetic calorimeter. For sufficiently hard muons, the information from the instrumented magnetic-flux return is also used. We correct for bremsstrahlung of electrons by combining the four-momentum of the electron with those of detected photons which are emitted close to the electron direction. We require lepton candidates to have a momentum in the CM frame $p^*_\ell > 0.35\ {\rm GeV}/c$ and a point of closest approach to the collision axis of less than 0.1 cm. The p^*_ℓ selection value is motivated by the large mass of the Λ_c^+ and the assumption of another baryon in the decay due to baryon number conservation, which greatly restricts the kinetic energy available to the leptons. We identify photon conversions and π^0 Dalitz decays using a dedicated algorithm based on the vertex and kinematic properties of two opposite charge tracks, and eliminate electron candidates coming from these.

Candidate Λ_c^+ baryons are reconstructed in the $pK^-\pi^+$, pK^0_S, $pK^0_S\pi^+\pi^-$, $\Lambda\pi^+$, and $\Lambda\pi^+\pi^+\pi^-$ modes. Λ candidates are reconstructed in the $p\pi^-$ decay mode. Only Λ_c candidates with opposite charge of the lepton candidate are considered. Charged daughters of the Λ_c^+ candidate are fit to a vertex tree [11], with K^0_S and Λ masses constrained to their known values [4], and the Λ_c^+ origin constrained to the known average luminous position of the beams within its measured size and uncertainties. In events with multiple Λ_c^+ and/or ℓ candidates, the candidates are fit to a common vertex, and the $\Lambda_c^+\ell^-$ pair with the highest vertex fit probability is selected.

We refine the selection of $B_{\rm tag}$ candidates by first removing those whose daughter particles are based on tracks already used to reconstruct the signal side Λ_c^+ or lepton and those charged $B_{\rm tag}$ candidates whose flavor is opposite that of the signal $\bar{B}$ candidate. We account for mixing effects by weighting B^0 and $\bar{B}^0$ tags according to the Λ_c charge, as described in Ref. [12]. In events with multiple $B_{\rm tag}$ candidates, we select the one reconstructed in the highest purity mode, where the purity is estimated for each $B_{\rm tag}$ decay chain using MC simulation as the ratio of signal over background events. When multiple candidates in the same event have the same $B_{\rm tag}$ mode, we select the one with the smallest $|\Delta E|$ value.

We reconstruct the CM missing momentum $\vec{p}_{\rm miss}$ by noting that $\vec{p}_{\rm miss} + \vec{p}_{\rm vis} = \vec{0}$ in the CM frame, where the visible momentum $\vec{p}_{\rm vis}$ is computed by summing the momentum vectors of the $B_{\rm tag}$, the Λ_c and ℓ candidates, plus any additional well-measured charged track or neutral cluster boosted to the CM frame. We require $|\vec{p}_{\rm miss}| > 0.2\ {\rm GeV}/c$ to remove background from hadronic $\bar{B} \to \Lambda_c^+ X$ decays in which all the particles in the X system have been reconstructed and one hadron is misidentified as a lepton. We compute the total observed charge of the selected events by adding the charges of all particles used in the $\vec{p}_{\rm miss}$ calculation, and require this to be zero. This reduces the background in the $B_{\rm tag}$ reconstruction due to missing particles.

Backgrounds are divided according to whether they contain a correctly reconstructed Λ_c^+ candidate. Those which contain such a candidate are called ''peaking background,'' while those that do not are called ''combinatorial background.'' The predictions from MC simulation of generic $B\bar{B}$ and continuum events show that the peaking background arises mainly from hadronic $\bar{B} \to \Lambda_c^+ X$ decays, where the Λ_c^+ is correctly reconstructed, and the lepton candidate is an electron from gamma conversions or π^0 Dalitz decays, or a hadron misidentified as a muon; we estimate $3.6 \pm 0.7_{\rm stat} \pm 0.7_{\rm syst}$ and $15.3 \pm 1.5_{\rm stat} \pm 1.4_{\rm syst}$ peaking background events for the electron and muon samples, respectively. The relatively large peaking background rate for the muon channel is due primarily to the low lepton momentum cut.

We determine the $\bar{B}$ semileptonic signal yield with a simultaneous unbinned maximum likelihood fit to the distribution of the Λ_c^+ invariant mass on both the electron and muon samples. The Λ_c^+ invariant-mass distribution is described by the sum of three probability density functions (PDFs) representing signal, peaking background, and combinatorial background. The functional forms of the PDFs are chosen based on simulation studies. The signal and peaking background contributions are modeled as Gaussian functions whose mean and width are fixed to the values obtained from a fit to the Λ_c^+ candidate mass spectrum in the $\bar{B} \to \Lambda_c^+ X$ data sample described below. The number of peaking background events is fixed to the prediction from MC simulations. The combinatorial $B\bar{B}$ and continuum backgrounds are modeled as a first-order polynomial, whose parameters are constrained by a fit to the Λ_c^+ invariant-mass sidebands, defined as the mass ranges from 2.23–2.26 and 2.31–2.34 GeV/c^2. The fit to the Λ_c^+ invariant mass is shown in Fig. 2, projected separately for the electron and muon samples. The corresponding yields are shown in Table I.

In order to reduce systematic uncertainties due to $B_{\rm tag}$ and Λ_c^+ reconstruction, the $\bar{B} \to \Lambda_c^+ X \ell^- \bar{\nu}_\ell$ branching fraction is measured relative to the inclusive $\mathcal{B}(\bar{B} \to \Lambda_c^+ X)$ branching fraction. To determine the inclusive yield, we start with the same $B_{\rm tag}$ sample used for the semileptonic selection. We reconstruct Λ_c^+ candidates as in the semileptonic case, choosing the candidate with the highest vertex probability

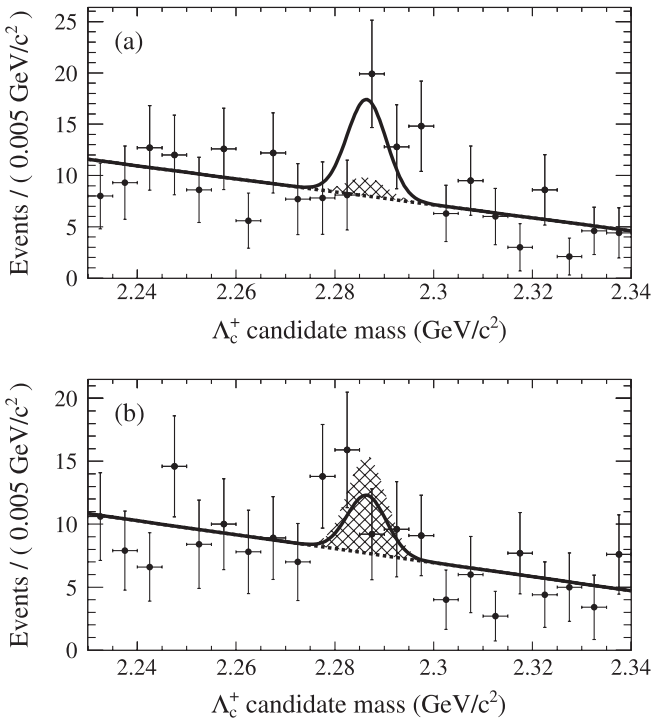

FIG. 2. Fit to the Λ_c^+ candidate mass distribution for $\bar{B} \to \Lambda_c^+ X e^- \bar{\nu}_e$ (a) and $\bar{B} \to \Lambda_c^+ X \mu^- \bar{\nu}_\mu$ (b). The data are shown as points with error bars, the overall fit as a solid line, and the peaking background contribution as a cross-hatched area. The combinatorial $B\bar{B}$ and continuum background is shown as the area below the dotted line.

in case of multiple candidates. We exclude $B_{\rm tag}$ candidates with daughter particles in common with the Λ_c^+ candidate and resolve multiple $B_{\rm tag}$ candidates as in the semileptonic case.

We determine the $\bar{B} \to \Lambda_c^+ X$ signal yield with an unbinned maximum likelihood fit to the Λ_c^+ invariant mass. The fit function consists of the sum of two PDFs representing signal and combinatorial backgrounds, described by a single Gaussian and a first-order polynomial, respectively. All parameters of the signal Gaussian are left free in the fit. We obtain a Λ_c^+ mass value of 2.2853 ± 0.0003 GeV$/c^2$, consistent with the current world average [4], and a resolution of 4.0 ± 0.3 MeV$/c^2$, consistent with expectations from MC simulations. The Λ_c^+ invariant-mass distribution on the inclusive sample and the results of the fit are shown in Fig. 3.

TABLE I. Signal yields and reconstruction efficiencies for the $\bar{B} \to \Lambda_c^+ X \ell^- \bar{\nu}_\ell$, $\bar{B} \to \Lambda_c^+ X$, and $B/\bar{B} \to \Lambda_c^+ X$ decays with the corresponding statistical uncertainties.

Decay mode	$N_{\rm data}$	$\epsilon(\times 10^{-5})$
$\bar{B} \to \Lambda_c^+ X e^- \bar{\nu}_e$	15.0 ± 6.8	1.98 ± 0.17
$\bar{B} \to \Lambda_c^+ X \mu^- \bar{\nu}_\mu$	-6.2 ± 6.3	1.04 ± 0.12
$\bar{B} \to \Lambda_c^+ X$	934 ± 55	3.09 ± 0.11
$B/\bar{B} \to \Lambda_c^+ X$	1386 ± 66	3.21 ± 0.12

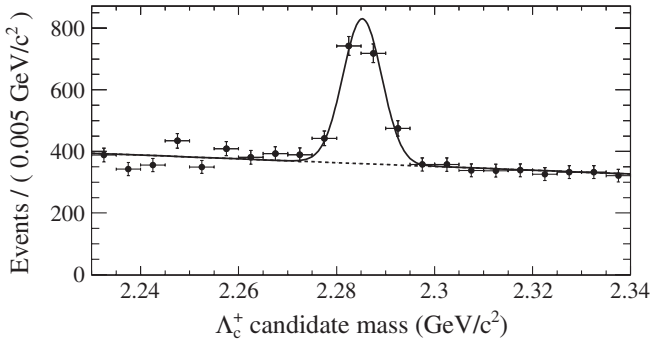

FIG. 3. Fit to the Λ_c^+ candidate mass distribution for $\bar{B} \to \Lambda_c^+ X$. The data are shown as points with error bars, the overall fit as a solid line, and the combinatorial $B\bar{B}$ and continuum background as a dashed line.

We determine the relative branching fraction $\mathcal{B}(\bar{B} \to \Lambda_c^+ X \ell^- \bar{\nu}_\ell)/\mathcal{B}(\bar{B} \to \Lambda_c^+ X)$ as the ratio of the measured signal yields, after correcting for the ratio of the reconstruction efficiencies:

$$\frac{\mathcal{B}(\bar{B} \to \Lambda_c^+ X \ell^- \bar{\nu}_\ell)}{\mathcal{B}(\bar{B} \to \Lambda_c^+ X)} = \left(\frac{N_{\rm s}}{N_{\rm i}}\right)\left(\frac{\epsilon_{\rm i}}{\epsilon_{\rm s}}\right). \quad (2)$$

Here, $N_{\rm s}$ ($N_{\rm i}$) is the number of $\bar{B} \to \Lambda_c^+ X \ell^- \bar{\nu}_\ell$ ($\bar{B} \to \Lambda_c^+ X$) events reported in Table I together with the corresponding reconstruction efficiencies $\epsilon_{\rm s}$ ($\epsilon_{\rm i}$); the latter include the $B_{\rm tag}$ efficiencies, which are estimated with MC simulation.

Many systematic uncertainties approximately cancel in this ratio, such as those due to the Λ_c^+ and $B_{\rm tag}$ reconstruction efficiencies and the Λ_c^+ decay branching fractions. We categorize the remaining systematic uncertainties into those which directly affect the signal yield, and those which affect only the efficiency. The systematic uncertainties that have been considered are described below and summarized in Table II.

Systematic uncertainties in the signal yield are dominated by the peaking background yield. We estimate this

TABLE II. Sources of systematic uncertainties.

Yield systematics (events)	$\ell = e$	$\ell = \mu$
Peaking background: sample statistics	1.0	1.4
Peaking background: $\mathcal{B}(\bar{B} \to \Lambda_c^+ X)$	1.6	4.7
Lepton mis-id rate	0.7	2.0
Fit bias	0.3	1.2
Total	2.0	5.4

Efficiency ratio systematics (%)	$\ell = e$	$\ell = \mu$
Signal model	11.3	35.9
Reco. efficiency statistics	8.4	11.4
Peaking background: $\bar{B} \to \Lambda_c^+ X$	1.9	1.9
Lepton id efficiency	1.1	2.7
Selection order	5.0	6.8
Total	15.1	38.4

by propagating the uncertainty in the $\bar{B} \to \Lambda_c^+ X$ branching fraction, and the Poisson error from the MC simulation. We add in quadrature the effect of varying the probability for a pion to be misidentified as an electron or as a muon by 15%, where the range is estimated using data control samples [10]. Systematic uncertainties due to background electrons from photon conversions and π^0 Dalitz decays are negligible.

To account for a possible bias due to the fit technique, we prepare ensembles of MC experiments, in which events are generated according to the PDF shapes determined from data. We vary the signal to background ratio and fit for the signal as in the full analysis. The average difference between the fitted value of the yield and the true value is taken as a systematic uncertainty, labeled "Fit bias" in Table II.

Systematic uncertainties on the reconstruction efficiency ratio are dominated by the uncertainty in the signal model. This is estimated by comparing our nominal signal model with a pure phase space model, where the $\bar{B} \to \Lambda_c^+ X \ell^- \bar{\nu}_\ell$ decay occurs in one step, taking the full difference in the signal efficiency estimate compared to our nominal signal model as the systematic uncertainty. The larger systematic uncertainty for the muon channel is due to the low muon identification efficiency for the soft leptons. The uncertainty in the reconstruction efficiency due to the limited statistics of the MC simulation is added as a systematic uncertainty by weighting the events to the data size. The peaking background in the inclusive mode due to $c\bar{c}$ is estimated using the prediction from our MC simulation and is found to be compatible with the statistical uncertainty of the sample, which we take as a systematic uncertainty. We estimate the systematic uncertainty on the signal efficiency due to particle identification by varying the electron (muon) identification efficiency by 2% (3%), based on studies using data control samples [10]. Since the order for selecting the best candidate is different between the semileptonic and inclusive samples, the uncertainties on the ratio of the $B_{\rm tag}$ and Λ_c^+ efficiencies do not exactly cancel. We evaluate the corresponding systematic uncertainty by reversing the order of the lepton and $B_{\rm tag}$ selection and comparing with our standard selection order using the same MC simulation of our signal model used to estimate the reconstruction efficiency. Since we find the reversed selection order efficiency to be compatible with the standard selection order efficiency within the precision of our MC simulation, we estimate the systematic uncertainty as the statistical uncertainty of that comparison.

The central values of the branching fraction ratios are summarized in Table III. We find a signal significance $\mathcal{S} = 2.1$, including the systematic uncertainties on the signal yields, from the difference in the log likelihood values between the nominal fit and a fit in which we fix the signal yield to zero. By scanning the likelihood values including the full systematic uncertainties, we estimate an upper limit at the 90% confidence level:

TABLE III. Central values of the branching fraction ratio $\mathcal{B}(\bar{B} \to \Lambda_c^+ X \ell^- \bar{\nu}_\ell)/\mathcal{B}(\bar{B} \to \Lambda_c^+ X)$. The last line averages over e and μ.

Mode	BF ratio
$\ell = e$	$2.5 \pm 1.1_{\rm stat} \pm 0.6_{\rm syst}$
$\ell = \mu$	$-2.0 \pm 2.0_{\rm stat} \pm 1.9_{\rm syst}$
$\ell = e, \mu$	$1.7 \pm 1.0_{\rm stat} \pm 0.6_{\rm syst}$

$$\frac{\mathcal{B}(\bar{B} \to \Lambda_c^+ X \ell^- \bar{\nu}_\ell)}{\mathcal{B}(\bar{B} \to \Lambda_c^+ X)} < 3.5\%. \quad (3)$$

For a comparison with the CLEO result [5], in which the flavor of the semileptonic B was not determined, we repeat the analysis without requiring the charge-flavor correlation between the $B_{\rm tag}$ and the Λ_c^+ in the inclusive mode. The corresponding yield for the inclusive mode is shown in the last row of Table I. We obtain the branching fraction ratio $\mathcal{B}(\bar{B} \to \Lambda_c^+ X \ell^- \bar{\nu}_\ell)/\mathcal{B}(B/\bar{B} \to \Lambda_c^+ X) = (1.2 \pm 0.7_{\rm stat} \pm 0.4_{\rm syst})\%$ with its corresponding 90% confidence level upper limit $\mathcal{B}(\bar{B} \to \Lambda_c^+ X \ell^- \bar{\nu}_\ell)/\mathcal{B}(B/\bar{B} \to \Lambda_c^+ X) < 2.5\%$, which improves the CLEO limit. We find that removing the charge-flavor correlation between the lepton and the $B_{\rm tag}$ in the semileptonic mode also yields consistent results after reestimating backgrounds.

In conclusion, we have presented a search for semileptonic B decays into the charmed baryon Λ_c^+. We obtain an improved upper limit with respect to previous measurements [5] on the relative branching fraction $\mathcal{B}(\bar{B} \to \Lambda_c^+ X \ell^- \bar{\nu}_\ell)/\mathcal{B}(\bar{B} \to \Lambda_c^+ X)$, which is found to be much smaller than the corresponding relative branching fraction for B decays into charmed mesons. Our result shows that the rate of baryonic semileptonic B decay is too small to contribute substantially to the branching fractions of inclusive semileptonic B decays.

We are grateful for the excellent luminosity and machine conditions provided by our PEP-II colleagues, and for the substantial dedicated effort from the computing organizations that support *BABAR*. The collaborating institutions wish to thank SLAC for its support and kind hospitality. This work is supported by DOE and NSF (U.S.), NSERC (Canada), CEA and CNRS-IN2P3 (France), BMBF and DFG (Germany), INFN (Italy), FOM (The Netherlands), NFR (Norway), MES (Russia), MEC (Spain), and STFC (United Kingdom). Individuals have received support from the Marie Curie EIF (European Union) and the A. P. Sloan Foundation.

[1] Charge conjugation is always implied unless stated otherwise.
[2] I. I. Y. Bigi, B. Blok, M. A. Shifman, and A. I. Vainshtein, Phys. Lett. B **323**, 408 (1994); G. Buchalla, I. Dunietz, and H. Yamamoto, Phys. Lett. B **364**, 188 (1995).
[3] B. Aubert *et al.* (*BABAR* Collaboration), Phys. Rev. Lett. **100**, 151802 (2008); P. del Amo Sanchez *et al.* (*BABAR* Collaboration), Phys. Rev. D **83**, 032004 (2011).
[4] K. Nakamura *et al.* (Particle Data Group), J. Phys. G **37**, 075021 (2010).
[5] G. Bonvicini *et al.* (CLEO Collaboration), Phys. Rev. D **57**, 6604 (1998).
[6] B. Aubert *et al.* (*BABAR* Collaboration), Nucl. Instrum. Methods Phys. Res., Sect. A **479**, 1 (2002).
[7] S. Agostinelli *et al.* (GEANT4 Collaboration), Nucl. Instrum. Methods Phys. Res., Sect. A **506**, 250 (2003).
[8] T. Sjostrand, Comput. Phys. Commun. **82**, 74 (1994).
[9] J. L. Goity and W. Roberts, Phys. Rev. D **51**, 3459 (1995).
[10] B. Aubert *et al.* (*BABAR* Collaboration), Phys. Rev. Lett. **92**, 071802 (2004).
[11] W. D. Hulsbergen, Nucl. Instrum. Methods Phys. Res., Sect. A **552**, 566 (2005).
[12] B. Aubert *et al.* (*BABAR* Collaboration), Phys. Rev. D **69**, 111104 (2004).